

AUTHOR QUERIES

Author Please Answer All Queries

AQ—Please note that all nonstandard abbreviations in your article have been spelled out per journal style (list of standard abbreviations available at: <http://anesthesiology.pubs.asahq.org/public/InstructionsforAuthors.aspx>).

AQ1—For indexing purposes, please confirm that author names have been correctly identified as given names (blue), surnames (red), and suffixes (black). Color in the byline will not appear on the final published version.

AQ2—Please confirm that the short title for your article is correct.

AQ3—Please confirm all author affiliations are accurate. Note: per journal style, affiliations must be in English. Please provide English translations if applicable.

AQ4—Please note that structured abstract should have the following headings: “Background; Methods; Results; Conclusions:” as per journal style. Hence, please amend the headings as needed.

AQ5—PE: The following summary statement was deleted from the article. Summary Statement: A target plasma concentration of 0.3 ng·mL⁻¹ would be reached within 20 min in 95% of the simulated individuals with intranasal dexmedetomidine at 2 µg·kg⁻¹, and an average peak concentration of 0.563 ng·mL⁻¹ would be attained at 61 min.

AQ6—“Caucasian” is generally not used in the literature. Change to “white” throughout the article?

AQ7—Please confirm the date “June 3, 2016.”

AQ8—Should “besilate” be “besylate”?

AQ9—Both ALT and AST were defined as “alanine aminotransferase.” Please check. “AST” should not be used in the article but was retained so that the correct definition can be inserted.

AQ10—Please provide a manufacturer and country for PopED.

AQ11—Is “1‰” correct?

AQ12—Manufacturer inserted for TSQ Quantum Ultra. Please confirm it is correct as listed.

AQ13—Please expand m/z. Please define the arrow symbols if possible.

AQ14—Please make sure all abbreviations in all equations are defined. Please make sure these abbreviations are formatted consistently throughout the article and tables. In the article and tables, Please spell out any nonstandard abbreviations that do not appear in the equations.

AQ15—Please list specific section rather than “above.”

AQ16—Please expand Emax unless it is part of an equation. Please expand CL unless it is part of a drug name.

AQ17—Please check all supplemental digital content links to confirm the material is correct

AQ18—Please clarify what value is meant by “5th–95th.”

AQ19—Should “CL/F” “V1/F” “Q/F” “V2/F” in Table 3 be italicized?

AQ20—The full figure legends have been added to the shorter legends originally provided in the manuscript. Nonstandard abbreviations for the journal should not appear in the legends and have been spelled out.

AQ21—Is the value 600 correct here?

AQ22—Should “27-month-old and 12.5 kg” be changed to “age 27 months and body weight 12.5 kg”?

AQ23—In Fig. 3, if appropriate, please change the “u” in “ug” to a “mu” symbol, meaning micrograms.

AQ24—Please expand PK.

AQ25—Please provide an academic degree for each person mentioned in the Acknowledgments.

AQ26—Please provide a city for each institution mentioned.

AQ27—Please confirm information in Reproducible Science section is correct.

AQ28—For ref. 15, please clarify the type of reference and provide complete publication information.

ANESTHESIOLOGY

Population Pharmacokinetics of Intranasal Dexmedetomidine in Infants and Young Children

Bi L. Li, M.D., Yan P. Guan, M.D., Vivian M. Yuen, M.D., Wei Wei, M.D., Min Huang, Ph.D., Ma Z. Zhang, M.D., Ai W. Li, Ph.D., Joseph F. Standing, Ph.D., Guo P. Zhong, Ph.D., Xing R. Song, M.D.

ANESTHESIOLOGY 2022; XXX:00–00

EDITOR'S PERSPECTIVE

What We Already Know about This Topic

- Intranasal dexmedetomidine is widely used for procedural sedation and as premedication for children

What This Article Tells Us That Is New

- Based on pharmacokinetic data in a cohort of children aged 3 months to 3 yr, intranasal dexmedetomidine $2 \mu\text{g} \cdot \text{kg}^{-1}$ would provide a therapeutic threshold of mild to moderate sedation lasting for up to 2 h

Intranasal dexmedetomidine is widely used in pediatric patients for procedural sedation¹ because it is easy and convenient to administer and is not associated with an

ABSTRACT

Background: Intranasal dexmedetomidine provides noninvasive, effective procedural sedation for pediatric patients, and has been widely used in clinical practice. However, the dosage applied has varied fourfold in pediatric clinical studies. To validate an appropriate dosing regimen, this study investigated the pharmacokinetics of intranasal dexmedetomidine in Chinese children under 3 yr old.

Methods: Intranasal dexmedetomidine $2 \mu\text{g} \cdot \text{kg}^{-1}$ was administered to children with simple vascular malformations undergoing interventional radiological procedures. A population pharmacokinetic analysis with data from an optimized sparse-sampling design was performed using nonlinear mixed-effects modeling. Clearance was modeled using allometric scaling and a sigmoid postmenstrual age maturation model. Monte Carlo simulations were performed to assess the different dosing regimens.

Results: A total of 586 samples from 137 children aged 3 to 36 months were included in the trial. The data were adequately described by a two-compartment model with first-order elimination. Body weight with allometric scaling and maturation function were significant covariates of dexmedetomidine clearance. The pharmacokinetic parameters for the median subjects (weight 10 kg and postmenstrual age 101 weeks) in our study were apparent central volume of distribution 7.55 l, apparent clearance of central compartment $9.92 \text{ l} \cdot \text{h}^{-1}$, apparent peripheral volume of distribution 7.80 l, and apparent intercompartmental clearance $61.7 \text{ l} \cdot \text{h}^{-1}$. The simulation indicated that at the dose of $2 \mu\text{g} \cdot \text{kg}^{-1}$, 95% of simulated individuals could achieve a target therapeutic concentration of $0.3 \text{ ng} \cdot \text{ml}^{-1}$ within 20 min, and the average peak concentration of $0.563 \text{ ng} \cdot \text{ml}^{-1}$ could be attained at 61 min.

Conclusions: The pharmacokinetic characteristics of intranasal dexmedetomidine were evaluated in Chinese pediatric patients aged between 3 and 36 months. An evidence-based dosing regimen at $2 \mu\text{g} \cdot \text{kg}^{-1}$ could achieve a preset therapeutic threshold of mild to moderate sedation that lasted for up to 2 h.

(ANESTHESIOLOGY 2022; XXX:00–00)

unpleasant sensation. Intranasal dexmedetomidine at $1 \mu\text{g} \cdot \text{kg}^{-1}$ is rapidly absorbed, with a sedation onset time of approximately 25 min in children² and 45 min in healthy adult

Supplemental Digital Content is available for this article. Direct URL citations appear in the printed text and are available in both the HTML and PDF versions of this article. Links to the digital files are provided in the HTML text of this article on the Journal's Web site (www.anesthesiology.org). B.L.L. and Y.P.G. contributed equally to this article. X.R.S. and G.P.Z. contributed equally to this article.

Submitted for publication June 11, 2021. Accepted for publication April 21, 2022.

Bi L. Li, M.D.: Department of Anesthesiology, Guangzhou Women and Children's Medical Center, Guangzhou Medical University, Guangzhou, China.

Yan P. Guan, M.D.: Institute of Clinical Pharmacology, School of Pharmaceutical Sciences, Sun Yat-Sen University, Guangzhou, China.

Vivian M. Yuen, M.D.: Department of Anesthesiology and Perioperative Medicine, Hong Kong Children's Hospital, Hong Kong, China.

Wei Wei, M.D.: Department of Anesthesiology, Guangzhou Women and Children's Medical Center, Guangzhou Medical University, Guangzhou, China.

Min Huang, Ph.D.: Institute of Clinical Pharmacology, School of Pharmaceutical Sciences, Sun Yat-Sen University, Guangzhou, China.

Ma Z. Zhang, M.D.: Department of Anesthesiology, Shanghai Children's Medical Center, Shanghai Jiao Tong University School of Medicine, Shanghai, China.

Ai W. Li, Ph.D.: Department of Pharmacology and Pharmacy, University of Hong Kong, Hong Kong, China.

Joseph F. Standing, Ph.D.: Great Ormond Street Institute of Child Health, University College London, London, United Kingdom.

Guo P. Zhong, Ph.D.: Institute of Clinical Pharmacology, School of Pharmaceutical Sciences, Sun Yat-Sen University, Guangzhou, China.; Phase I Clinical Trial Center, Sun Yat-Sen Memorial Hospital, Sun Yat-Sen University, Guangzhou, China.

Xing R. Song, M.D.: Department of Anesthesiology, Guangzhou Women and Children's Medical Center, Guangzhou Medical University, Guangzhou, China.

Copyright © 2022, the American Society of Anesthesiologists. All Rights Reserved. Anesthesiology 2022; XXX:00–00. DOI: 10.1097/ALN.0000000000004258

PERIOPERATIVE MEDICINE

volunteers.^{3,4} It is associated with a good safety profile, with only mild hemodynamic changes and minimal respiratory depression.^{5,6}

As clinical evidence accumulates supporting the therapeutic effect evaluation of intranasal dexmedetomidine in pediatric subjects, the importance of understanding the pharmacokinetic and time-concentration profiles at different doses increases to minimize adverse reactions and facilitate clinical decision-making. The therapeutic effect of intranasal dexmedetomidine in children has been extensively studied; however, the pharmacokinetic profile has not been sufficiently described. To date, only two intranasal dexmedetomidine pharmacokinetic studies on a small number of children have been reported. These include a study of 13 Chinese children aged 4 to 10 yr and another study on 18 African-American and Caucasian children aged 6 to 48 months.^{7,8} Neither of these studies used their models to simulate optimal dosing. Potts *et al.* reported reduced clearance in infants and their simulation based on a two-compartment model with sigmoidal maturation and allometric models.⁹ They suggested that children were aroused from sedation at a plasma concentration of $0.304 \text{ ng} \cdot \text{ml}^{-1}$ after an infusion of dexmedetomidine. Our current study assessed the pharmacokinetic profile of intranasal dexmedetomidine administration in a large cohort of relatively healthy children under 3 yr old with simple vascular malformations. Moreover, plasma concentration-time profiles with different dosing regimens and age groups were characterized by simulation.

Materials and Methods

This prospective pharmacokinetic study was approved by the Guangzhou Women and Children's Medical Center (Guangzhou, China) Review Board (Institutional Review Board 201507) and registered before the first patient enrollment at the Chinese Clinical Trial Registry (ChiCTR-OPC-16008589, Principal investigator: B. L. Li, Date of registration: June 3, 2016).

Written informed consent was obtained from all the guardians of the subjects recruited in this study before surgery. This study adhered to the revised Declaration of Helsinki of the World Medical Association (Ferney-Voltaire, France) and International Conference on Harmonization and Good Clinical Practice Guidelines.

Study Population

Subjects were enrolled from June 2016 to November 2017 at the Guangzhou Women and Children's Medical Center. We enrolled children between 3 and 36 months of age, American Society of Anesthesiologists (Schaumburg, Illinois) Physical Status I and II, with simple vascular malformations as classified by the International Society for the Study of Vascular Anomalies (Milwaukee, Wisconsin) Criteria, and requiring intervention radiological procedures. The exclusion

criteria included a history of allergy or hypersensitivity to dexmedetomidine; severe hepatic impairment; hematological, cardiovascular, endocrine, metabolic, and gastrointestinal diseases; exposure to dexmedetomidine or any other sedative within a week; and the presence of active respiratory symptoms, rhinorrhea, and vascular malformations in or near the nasal cavity that might influence nasal drug absorption.

Clinical Protocol

All subjects received $2 \text{ mg} \cdot \text{kg}^{-1}$ propofol, $0.3 \text{ } \mu\text{g} \cdot \text{kg}^{-1}$ sufentanil, and $0.2 \text{ mg} \cdot \text{kg}^{-1}$ cisatracurium besilate at anesthesia induction and had laryngeal mask airway placement or tracheal intubation. After intravenous induction of anesthesia, intranasal dexmedetomidine at $2 \text{ } \mu\text{g} \cdot \text{kg}^{-1}$ was administered. Undiluted preservative-free dexmedetomidine ($100 \text{ } \mu\text{g} \cdot \text{ml}^{-1}$; Ai Bei Ning, JiangSu Singchn Pharmaceutical Co. Ltd., China) was used. The solution was drawn into a 1-ml tuberculin syringe and attached to a mucosal atomization device (MAD Nasal, Teleflex Incorporated, USA). The dead space of the atomization device was approximately 0.15 ml, and it was primed with dexmedetomidine so that exactly $2 \text{ } \mu\text{g} \cdot \text{kg}^{-1}$ dexmedetomidine was drawn to the tuberculin. An equal volume of the drug was administered to each nostril of the participants. A single pediatric anesthesiologist (B.L. Li) with extensive experience using the atomizer device performed all nasal dexmedetomidine administrations. General anesthesia was maintained with sevoflurane. Intranasal administration at 2 to $3 \text{ } \mu\text{g} \cdot \text{kg}^{-1}$ dexmedetomidine is commonly used for procedural sedation.^{6,10} To prevent interventional puncture site rebleeding caused by postoperative emergence agitation,¹¹ we used intranasal dexmedetomidine at $2 \text{ } \mu\text{g} \cdot \text{kg}^{-1}$ as an adjuvant for anesthesia. Vital signs, including oxygen saturation measured by pulse oximetry (SpO_2), pulse rate, noninvasive systolic blood pressure (SBP), and sedation score (University of Michigan Sedation Score), were measured at baseline and every 5 min until the discharge criteria were reached. Pulse rate and noninvasive SBP were recorded when their values were lower or higher than 20% of the age-defined normal range limits. Hypoxia was defined as SpO_2 equal to or less than 93%.

The following clinical data were collected and evaluated as covariates due to their potential influence on dexmedetomidine pharmacokinetics: postnatal age,¹² postmenstrual age (defined as the sum of gestational and postnatal age), weight, sex, albumin, bilirubin, hemoglobin, glucose, liver function (alanine aminotransferase and alanine aminotransferase [AST]), creatinine, creatinine clearance,¹³ and coadministered drugs.

Blood Sampling and Drug Determination

The dexmedetomidine sampling strategy adopted herein was designed according to the D-optimal criterion using

AQ8

AQ9

AQ10

PopED in the R language. Pharmacokinetic parameters of intranasal dexmedetomidine from healthy adult subjects were extrapolated to children based on allometric scaling.⁴ Sampling windows were estimated around each sampling time to ensure that the design was clinically feasible. The D-optimality product criterion was evaluated using the following parameters: Fisher information matrix, normalized efficiency, and coefficients of variation. The final blood sampling schedule by age was as follows: 3- to 12-month-old subjects (Group 1), 13- to 23-month-old subjects (Group 2), and 24- to 36-month-old subjects (Group 3) at 6, 18, 120, 180, and 360 min; 6, 18, 60, 240, and 360 min; and 6, 18, 120, 240, and 360 min, respectively, with a minimal subject number of 50 in total. Subsequently, a 1-ml blood sample was collected from an indwelling intravenous cannula into heparin sodium tubes. After collection, the samples were centrifuged at 4°C for 10 min at 3,000 rpm · min⁻¹ and then stored at -80°C until analysis.

Bioassay

Plasma dexmedetomidine concentrations were quantified by validated ultrahigh-performance liquid chromatography–tandem mass spectrometry using a stable isotope-labeled internal standard.¹⁴

The dexmedetomidine concentration in plasma was analyzed using a ultrahigh-performance liquid chromatography system (Thermo Fisher Scientific Inc., USA) consisting of an Ultimate 3000 RSLC system with binary pumps and an S surveyor autosampler (Thermo Fisher Scientific Inc.) coupled with a TSQ Ultra triple-quadrupole mass spectrometer (Thermo Fisher Scientific Inc.). Samples were separated on an Acquity BEH C₁₈ column (2.1 mm × 50 mm, 1.7 μm particle size; Waters, USA) set at 40°C. The mobile phase consisted of acetonitrile (A) and 1% formic acid water solution (B) at a flow rate of 0.3 ml · min⁻¹. The total run time of each sample was 3.1 min. The conditions of the gradient elution were set as follows: 0 to 0.5 min, 28% A; 0.5 to 1.5 min, 28 to 90% A; 1.5 to 2.0 min, 90% A; 2.0 to 2.1 min, 90 to 28% A; and 2.1 to 3.1 min, 28% A.

AQ11

Mass spectrometric detection was performed on a TSQ Quantum Ultra triple-quadrupole mass spectrometer (Thermo Fisher Scientific Inc.) equipped with an electrospray ionization interface. Dexmedetomidine and deuterated medetomidine were monitored under positive ion-switching electrospray ionization conditions and quantified in the selected reaction monitoring mode with transitions of m/z 201.3 → 95.1 and 204.2 → 98.0, respectively.

AQ12

The ultrahigh-performance liquid chromatography–tandem mass spectrometry method was validated with a lower limit of quantification of 0.05 ng · ml⁻¹. The linear range was 0.05 to 10 ng · ml⁻¹ (r² > 0.99) for dexmedetomidine. The within-batch and between-batch precision levels were less than 7.67%, whereas the accuracy ranged from -3.06 to 11.2%. The bioassay was fully validated according to the Food and Drug Administration (Silver Spring, Maryland)

AQ13

Guidelines.¹⁵ The bioassay showed good linearity, acceptable precision and accuracy, negligible matrix effects, and excellent extraction efficiency.

Pharmacokinetic Modeling

The concentration–time data for dexmedetomidine were modeled by first-order conditional estimation with interaction using the nonlinear mixed-effect modeling program Phoenix NLME (Version 7.0, Certara L.P. Pharsight, USA).

The clinical team recorded the precise drug administration and sampling time using dedicated bedside reporting documentation and then transcribed them into a case report form. Missing observations or concentration data were excluded from the analysis. Missing covariate values were replaced by previous values recorded before surgery from the same individual or interpolated for time-dependent covariates. The rest, if not resolved, was replaced with the median value from the study population.¹⁶ Concerning the management of plasma concentrations below the quantification limit the m³ Method was used to fit the pharmacokinetics model.¹⁷ The m³ method allowed the below the quantification limit observations to be retained but handled them as censored observations under the assumption that all the concentrations were normal. The likelihood for all the data to be maximized with respect to the model parameters, and the likelihood for a below the quantification limit observation in particular, were taken to be the likelihood that the observation was indeed below the quantification limit.¹⁷

Model Building

By visually inspecting the raw data and reviewing the literature, it was deemed likely that a one- or two-compartment disposition model would suffice, with a possible need for an absorption lag. Therefore, one- or two-compartment open models were compared, and each model had first-order absorption with or without a lag time to describe the absorption phase. The interindividual variabilities were assumed to follow log-normal distributions (η on CL/F , η on Q/F , η on V_1/F and V_2/F with covariance) and were implemented in the base model as (equation 1)

AQ14

$$P_i = P_{pop} \star \exp(\eta_i) \quad (1)$$

where P_i is the estimated pharmacokinetic parameter value for the i^{th} subject. P_{pop} is the mean pharmacokinetic parameter, and η_i is the interindividual variability between the log-transformed individual-specific parameter and a typical parameter. Independent and identically distributed random variables were normally distributed around 0 with variance ω^2 and the variable i for the i^{th} individual.

The models were parameterized using the first-order absorption rate (Ka), apparent central volume of distribution (V_1/F), apparent peripheral volume of distribution (V_2/F), apparent clearance of central compartment (CL/F),

PERIOPERATIVE MEDICINE

apparent clearance of peripheral compartment (Q/F), and lag time.

A combined proportional and additive model was evaluated to estimate the residual variability based on a visual inspection of the routine diagnostic plots and improvement of the objective function value. The residual variability is expressed as $Cm_{ij} = C_{pij} + C_{pij} \cdot \varepsilon_{prop,ij} + \varepsilon_{add,ij}$, where Cm_{ij} is the j^{th} observed concentration of the i^{th} subject, C_{pij} is the j^{th} model-predicted concentration of the i^{th} subject, and $\varepsilon_{prop,ij}$ and $\varepsilon_{add,ij}$ are the random variables with a mean of zero and variance $\sigma_{prop,ij}^2$ and $\sigma_{add,ij}^2$. The residual variability in sample collection, analytical determination, and model-misspecification risk might result in estimated variance (σ^2).¹²

Covariate Analysis

Demographic characteristics, such as age, weight, and liver function (alanine aminotransferase, AST), could serve as covariates and could be used to investigate their influences on pharmacokinetics.¹⁸

The allometric power models related to pharmacokinetic parameters are represented in equation 2 and equation 3,

$$F_{size} = \left(\frac{\text{Weight}}{\text{Weight}_{median}} \right)^{\text{coefficient}} \quad (2)$$

where F_{size} is the fractional difference in allometrically scaled size compared to an individual with a median weight, weight_{median} is the standard median weight of the study population, and the coefficient is an empirically derived constant; and

$$F_{size} = \left(\frac{\text{Weight}}{70\text{kg}} \right)^{\text{coefficient}} \quad (3)$$

where F_{size} is the fractional difference in allometrically scaled size compared to an individual with a weight of 70 kg. Weight represents an individual's body weight (i), and 70 kg is the standard adult body weight. For both allometric models described above, apparent peripheral clearance and volume of distribution were standardized with a body weight of 70 kg or median weight using the allometric coefficients of 0.75 for clearance and 1 for distribution.¹⁸

Collinearity of age and size is a fundamental feature, but they are not mutually exclusive.¹⁹ Age-dependent changes in body weight affecting drug disposition should also be considered.²⁰ After examining the influence of body weight on the basic model, a sigmoid Emax model was tested to account for differences in body size and maturation function of dexmedetomidine CL on postmenstrual age.¹² The model allows gradual maturation of clearance in the early life stage (equation 4),¹⁸

$$F_{mat} = \left(\frac{PMA^\gamma}{PMA^\gamma + TM_{50}^\gamma} \right) \quad (4)$$

where F_{mat} is the fraction of adult dexmedetomidine clearance value, TM_{50} is the postmenstrual age at which the clearance is 50% of the mature value, and γ is the Hill coefficient for clearance.

Clearance (CL/F) could then be described as follows (equation 5):

$$CL / F = CL_{pop} * F_{size} * F_{mat} * \exp(\eta_i) \quad (5)$$

where CL_{pop} is the population estimated value of clearance.

After delineating size and age, the forward and inclusion-backward elimination method was performed to analyze other potential covariates in the nested model. In the forward step of the covariate screening period, a covariate was included if the best improvement in the goodness-of-fit was found, and a statistically significant decrease of at least 10.60 in objective function value ($P < 0.005$, with 1 degree of freedom) was obtained. Subsequently, all significant covariates were added. The backward deletion was performed using a stringent statistical significance of $P < 0.001$ to preserve the influenced covariates in the final model for an increase in objective function value of greater than 13.82 (with 1 degree of freedom). Model convergence, reasonable estimates of parameter values, and precision were also considered for covariate selection.

Model Evaluation

A nonparametric bootstrap resampling method was applied to evaluate the stability and performance of the final model. The original dataset was resampled at the subject level to generate 1,000 new datasets. The 1,000 resampled datasets were used to obtain the 2.5th and 97.5th percentiles of the simulated model parameters. If the model was valid, the parameter estimates derived from the original dataset were similar to the median and were included in the 2.5th and 97.5th percentiles. The final model was evaluated using a prediction-corrected visual predictive check.²¹ This method generated virtual predictions and observations based on some values obtained by Monte Carlo simulations. The percentiles of the simulated data were compared with the corresponding percentiles of the observed data.

Model Simulation

A wide range of intranasal dosages was reported to be used in children;²² the most commonly reported dose was 1 to 4 $\mu\text{g} \cdot \text{kg}^{-1}$.^{23,24} Therefore, the pharmacokinetic profiles at dosage regimens of 1 to 4 $\mu\text{g} \cdot \text{kg}^{-1}$ for children (postmenstrual age, 101 weeks; weight, 10 kg) were simulated *via* Monte Carlo simulations. All the children in the simulation were assumed to be term births with a gestational age of 40 weeks. For each scenario, 1,000 replications were performed. The time-concentration profiles for the male term children whose ages ranged from 3 months to 3 yr (3, 6, and 9 months, and 1, 2, and 3 yr) were also simulated. Clinical covariates were based on the 50th percentile

weight estimates per age for boys as provided by the Clinical Growth Charts from Chinese children references.²⁵

Statistical Analysis

Model building was conducted using Phoenix NLME (Version 7.0, Certara L.P. Pharsight). Graphs were prepared using GraphPad Prism 8 (GraphPad Software Inc., USA). The patients' characteristics were summarized as the median (interquartile range) and range of observations, whichever was appropriate. All model parameters are reported as estimated values with relative standard errors. A two-tailed unpaired *t* test was performed to compare the time to reach the maximum plasma concentration (T_{max}) and the maximum concentration (C_{max}) between different age groups by simulated intranasal dexmedetomidine values. The results were analyzed using $P < 0.05$ for statistical significance.

Results

Study Population

A total of 140 Chinese children were recruited from June 9, 2016, to November 9, 2017. Three patients dropped out of the study because of the cancellation of scheduled surgery; thus, 137 children completed the study and were included in the analysis. The demographic information is summarized in table 1.

Safety Outcome

The median (interquartile range) duration of anesthesia was 30.0 min (24.0 to 44.5 min). The median (interquartile range) wake-up time (from anesthesia start to the time to reach University of Michigan (Ann Arbor, Michigan) Sedation Score [0 to 1]) was 43.5 min (32.5 to 55.8 min),

and the median (interquartile range) time for the patients to be discharged to the ward after anesthesia was 50 min (35 to 65 min). Eight patients experienced hypotension during the operation, and one 33-month-old patient required epinephrine to treat hypotension after his SBP fell to 58 mmHg. No episodes of oxygen desaturation, bradycardia, or hypertension occurred.

Pharmacokinetic Model Building

There were 685 scheduled blood sample collections; however, the investigator failed to collect 37 blood samples because of other clinical commitments. An additional 45 samples were missed due to blocked cannula, and 17 samples were not collected because of parental refusal. In total, 586 samples were included in the final analysis, and all the included samples were taken within the effective window of each optimal sampling schedule. For the concentration data below the lower limit of quantification, a likelihood-based approach was applied where lower limit of quantification data were flagged and treated as categorical data.^{17,26} In this study, 32 (5.46%) plasma concentrations were below the quantification limit, and the values for below the quantification limit observations that were considered normally distributed were replaced by random values somewhere between negative infinity and the lower limit of quantification.²⁶ The plasma concentrations of dexmedetomidine over time for the three groups divided by age (3- to 12-month-old subjects in Group 1, 13- to 23-month-old subjects in Group 2, and 24- to 36-month-old subjects in Group 3) are presented in Supplemental Digital Content 1 (<http://links.lww.com/ALN/C857>). The measured concentrations and individual/population predictions *versus* time are shown in Supplemental Digital Content 2 and 3 (<http://links.lww.com/ALN/C858>, <http://links.lww.com/ALN/C859>).

A two-compartment model described intranasal dexmedetomidine pharmacokinetics with first-order elimination from the central compartment. Adding the second compartment yielded a smaller improvement in fit than that yielded from the one-compartment model (Δ objective function value, -4.6 ; diagnostic plots shown in Supplemental Digital Content 4 (<http://links.lww.com/ALN/C860>). Although the objective function value improvement was minor, the two-compartment model was still selected. The reasons were that the one-compartment model exhibited larger errors and interindividual variances concerning the associated pharmacokinetic parameters (17 to 122%) and showed poorer diagnostic plots when compared with the two-compartment model.

The basic models were estimated with or without lag time ($-2LL = -681.3$, if the lag time was absent). Different lag times were also compared (data not shown); the lag times were fixed at 0.5 min (Δ objective function value, -80.3) and 5 min (Δ objective function value, -150.3) but with V_1/F lower than 10 l, and 10 min (Δ objective function value, 424.3). Finally, the basic model with an estimated

Table 1. Subject Characteristics

Characteristic	Value
No. of Patients	137
Sex, female/male	63/74
Premature, yes/no	5/132
Postnatal age, mo	14 (8–23 [3–36])
Postmenstrual age, wk	101 (75–140 [53–205])
Body weight, kg	10 (8–11.6 [5–17])
Height, cm	76 (68–87 [53–102])
Creatinine, $\mu\text{mol} \cdot \text{l}^{-1}$	20 (16–23 [10–63])
Creatinine clearance, $\text{ml} \cdot \text{min}^{-1}$	112 (102–125 [44–214])
No. of samples per patient	5 (4–5 [1–5])
Diagnosis classification	
Lymphatic malformations	59 (43.1%)
Venous malformations	25 (18.2%)
Arteriovenous malformations	22 (16.1%)
Arteriovenous fistula	31 (22.6%)

Data presented as median (interquartile range [range]) or number (proportion). Creatinine clearance calculated by Schwartz equation.

PERIOPERATIVE MEDICINE

lag time of 1.62 min (Δ objective function value, -12.8) fit the data. Given that the estimate of the proportional residual error ($\sigma^2_{prop, ij}$) asymptotically approached zero, this type of error was removed from the model, and only the additive model ($\sigma^2_{add, ij}$) was retained (model 3 and model 4 in table 2).

Covariate Analysis

The weight-based allometric method (standardization for a 70-kg adult, equation 3) was applied to the structural model (allometric coefficients of 0.75 for CL/F and Q/F and 1 for V_1/F and V_2/F), which caused a slight decrease in objective function value (Δ objective function value, -11.2). By comparison, a linear weight-normalized model with standardization for median weight yielded no improvement compared with that in the model standardized for a weight of 70 kg (Δ objective function value, 24.3). The addition of maturation of dexmedetomidine clearance based on postmenstrual age improved the model to an even greater extent than a 70-kg standardization allometric model (Δ objective function value, -96.9). The maturation parameters for clearance were estimated as follows: $TM_{50} = 44.7$ (coefficient of variation percentage, 17.3%) and $\gamma = 2.96$ (coefficient of variation percentage, 10.7%). Moreover, gestational age and postnatal age alone or together were not superior to postmenstrual age alone after adding to clearances (CL/F) and volumes ($V_1/F, V_2/F$), and other covariates (sex, creatinine, AST, and alanine aminotransferase) were not statistically justified when they were incorporated into the model. The description of the covariate analyses is provided in table 2.

Model diagnostics indicated acceptable goodness-of-fit for the final model (fig. 1). Finally, the model was best described by a two-compartment model with first-order elimination, an allometric scaling with estimates standardized to 70-kg weight, and maturation of clearance. The parameter estimates for the intranasal dexmedetomidine population pharmacokinetic model and bootstrap results are presented in table 3.

Model Validation

The reliability and stability of the final model were verified by bootstrapping (table 3) and prediction-corrected visual predictive check (fig. 2). The median of the bootstrap fixed-effects parameter estimates was within 5% of the population estimates from the original dataset for all parameters. The final model revealed a good fit between the predicted and observed dexmedetomidine concentrations, and the 5th, 50th, and 95th prediction intervals simulated from the posterior distribution of the final model parameter estimates were overlaid with the 5th, 50th, and 95th percentiles from the observed data.

Model Simulation

Intranasal dexmedetomidine pharmacokinetics were best described by the two-compartment model incorporating weight and postmenstrual age. The simulated concentration-time curves of the dose regimens across 1 to 4 $\mu\text{g} \cdot \text{kg}^{-1}$ are plotted in fig. 3, A and B. The plasma concentration curves for an intranasal dose at 2 $\mu\text{g} \cdot \text{kg}^{-1}$ were simulated in different typical boys with the 50th percentile estimates

Table 2. Stepwise and Objective Function Values Used for Discrimination

	Model	Pharmacokinetic Parameters	Reference Model	Objective Function Value
Structure model				
One-compartment model with first-order absorption, $\sigma^2_{prop, ij}$, $\sigma^2_{add, ij}$ *	1	$CL/F, V_1/F, Ka$		-676.7
Two-compartment model with first-order absorption, $\sigma^2_{prop, ij}$, $\sigma^2_{add, ij}$ *	2	$CL/F, V_1/F, Q/F, V_2/F, Ka$	1	-681.3
Two-compartment model with first-order absorption with lag time ($Tlag = 1.62$ min), $\sigma^2_{prop, ij}$ ($=0$), $\sigma^2_{add, ij}$ *	3	$CL/F, V_1/F, Q/F, V_2/F, Ka$	2	-693.2
Two-compartment model with first-order absorption with lag time ($Tlag = 1.62$ min), $\sigma^2_{add, ij}$ *	4	$CL/F, V_1/F, Q/F, V_2/F, Ka$	3	-693.9
Covariate model				
Weight-based allometric model				
70-kg weight-normalized model	5	$CL/F, V_1/F, Q/F, V_2/F$	4	-705.1
Weight-normalized model†	6	$CL/F, V_1/F, Q/F, V_2/F$	4	-680.8
Maturation model				
Postmenstrual age†	7	CL/F	5	-802.0
Postnatal age†	8		5	-772.1
Gestational age†	9		5	-710.8
Gestational age, postnatal age†	10		5	-780.8

Models 1 to 4 were base models without any covariates. Potential covariates (including weight, postmenstrual age, and postnatal age) were included to assess the covariate effect in models 5 to 10.

* $\sigma^2_{prop, ij}$ the estimated variance of the j^{th} observed concentration of the i^{th} subject by using a proportional error model; $\sigma^2_{add, ij}$ the estimated variance of the j^{th} observed concentration of the i^{th} subject by using an additive error model. †The covariates are centered on their median as $P_i = P_{pop} * (\text{Covariate} / \text{Median}(\text{Covariate}))^{\text{coefficient}}$, where $\text{Median}(\text{Covariate})$ is the median value of the covariate in the study population and coefficient quantifies the influence of the covariate on P_{pop} .

CL/F , apparent clearance of central compartment; Ka , first-order absorption rate; Q/F , apparent clearance of peripheral compartment; V_1/F , central volume of distribution; V_2/F , peripheral volume of distribution.

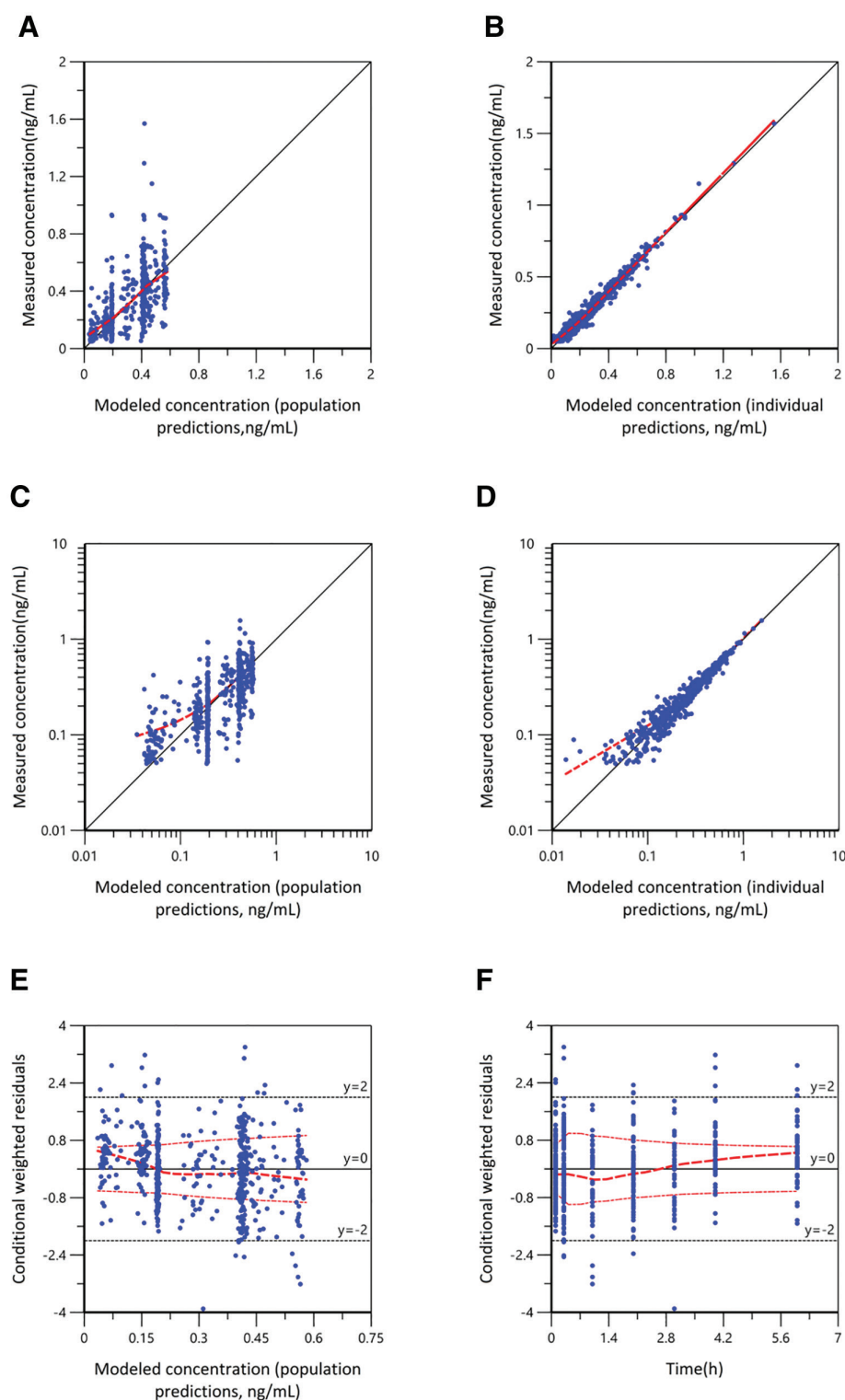


Fig. 1. Diagnostic scatter plots of the final model. Measured concentration *versus* the modeled concentration (population predictions; A) and *versus* modeled concentration (individual predictions; B). Log-log scaled plots of the measured concentration *versus* the modeled concentration (population predictions; C) and *versus* modeled concentration (individual predictions; D). Conditional weighted residuals *versus* modeled concentration (population predictions; E) and *versus* time (F). Red lines in A to D represents referenced lines ($y = x$). Both the thick and thin red lines in E and F represent the trend of the residual distribution. The thick red lines are fitted by locally weighted regression. The thin red line above zero is the smooth of the absolute values of the weighted residuals; the thin red line below zero is the mirror image.

AQ20

Table 3. Parameter Estimates for the Intranasal Dexmedetomidine Population Pharmacokinetic Model and Bootstrap Results

Pharmacokinetic parameters*	Estimates (RSE%)	BSV%	Bootstrap	
			Median	5th–95th
CL/F (L/h/[WT/70] ^{0.75})†	53.0 (11.1%)	42.7%	52.2 (6.0%)	46.7–58.1
V ₁ /F (L/[WT/70])	57.5 (17.5%)	46.3%	57.4 (3.1%)	11.1–115.2
Q/F (L/h/[WT/70] ^{0.75})	243.8 (24.5%)	21.4%	243.5 (21.1%)	62–300
V ₂ /F (L/[WT/70])	71.8 (12.3%)	27.3%	70.2 (20.5%)	24.8–95.7
K _a (h ⁻¹)	1.5 (10.1%)	59.2%	1.5 (23.2%)	0.5–2.3
TM ₅₀ (wk)	44.7 (17.3%)	—	45.1 (10.5%)	37.9–57.5
γ	3.0 (10.7%)	—	3.0 (18.8%)	2.4–9.2
Tlag (h)	0.03 (5.8%)	36.0%	0.03 (37.7%)	0.02–0.06
Interindividual variability (ω ²)				
CL/F	0.18 (2.9%)	—	0.16 (3.3%)	—
V ₁ /F	0.21 (11.7%)	—	0.26 (10.9%)	—
Q/F	0.04 (3.3%)	—	0.04 (2.1%)	—
V ₂ /F	0.07 (3.0%)	—	0.14 (15%)	—
K _a	0.35 (7.4%)	—	0.30 (9.5%)	—
TM ₅₀	—	—	—	—
γ	—	—	—	—
Tlag	0.12 (3.1%)	—	0.19 (16.2%)	—
Additive error (μg · ml ⁻¹)	0.05 (5.8%)	—	0.05 (9.5%)	0.04–0.06

*CL/F, apparent clearance of central compartment (allometrically scaled with exponent factor of 0.75 and a sigmoid hyperbolic maturation function of postmenstrual age); V₁/F, apparent central volume of distribution (allometrically scaled with exponent factor of 1); Q/F, apparent clearance of peripheral compartment (allometrically scaled with exponent factor of 0.75); V₂/F, apparent peripheral volume of distribution (allometrically scaled with exponent factor of 1); K_a, first-order absorption rate; TM₅₀, the postmenstrual age at which clearance is 50% that of the mature value; γ, the Hill coefficient for clearance; Tlag, lag time; ω, inter-individual variabilities of estimated parameters.

†Individual clearance of central compartment has an additional “maturation factor” and the estimate can be calculated by the following equation:

$$CL / F = CL_{pop} * \left(\frac{Weight}{70} \right)^{0.75} * \left(\frac{PMA^\gamma}{PMA^\gamma + TM_{50}^\gamma} \right) * \exp(nCL); V_1 / F = V_{pop} * \left(\frac{Weight}{70} \right)^1 * \exp(nV); Q / F = Q_{pop} * \left(\frac{Weight}{70} \right)^{0.75} * \exp(nQ); V_2 / F = V_{2pop} * \left(\frac{Weight}{70} \right)^1 * \exp(nV_2).$$

of weight per age reported in the Clinical Growth Charts for Chinese children.²⁵ The age (including postmenstrual age) and weight of each group were set as follows: (A) a 3-month-old child (postmenstrual age, 53 weeks; body weight, 6.8 kg), (B) a 6-month-old child (postmenstrual age, 66 weeks; body weight, 8.4 kg), (C) a 9-month-old child (postmenstrual age, 79 weeks; body weight, 9.3 kg), (D) a 1-year-old child (postmenstrual age, 92 weeks; body weight, 10.1 kg), (E) a 2-year-old child (postmenstrual age, 144 weeks; body weight, 12.5 kg), (F) a 3-year-old child (postmenstrual age, 196 weeks; body weight, 14.7 kg) (fig. 3C). The terminal half-life parameters of each group were 1.8 ± 0.8 h, 1.6 ± 0.7 h, 1.5 ± 0.6 h, 1.5 ± 0.7 h, 1.5 ± 0.8 h, and 1.5 ± 0.8 h, respectively. Ninety-five percent of the simulated individuals who received 2 μg · kg⁻¹ intranasal dexmedetomidine would achieve the target concentration of 0.3 ng · ml⁻¹ within 20 min. There was no significant difference in the T_{max} (P = 0.056) or the C_{max} among the different age groups (P = 0.721). A comparison between the pharmacokinetic parameters of intranasal dexmedetomidine is summarized in table 4.

Discussion

The current study described the pharmacokinetics of intranasal dexmedetomidine in a large cohort of Chinese children aged 3 months to 3 yr. Using an optimal sampling method combined with nonlinear mixed-effects analysis

and simulation, we demonstrated that a target plasma concentration of 0.3 ng · ml⁻¹ would be reached within 20 min in 95% of the simulated individuals treated with intranasal dexmedetomidine at 2 μg · kg⁻¹, and the C_{max} at 0.563 ng · ml⁻¹ would be attained at 61 min.

Given the paucity of relevant literature, comprehensive information on the pharmacokinetic profiles of intranasal dexmedetomidine administration in pediatric populations, especially among infants and young children, is still lacking. To date, only two studies based on small sample sizes have reported the pharmacokinetics of intranasal dexmedetomidine administration in this population. One focused on the peak plasma concentration in 18 African-American and Caucasian children aged 6 to 48 months,⁸ and the other conducted pharmacokinetic modeling of 13 Chinese children aged 4 to 10 yr.⁷ Miller *et al.* found that the average C_{max} values were 0.199 ng · ml⁻¹ and 0.355 ng · ml⁻¹ after intranasal administration of 1 and 2 μg · kg⁻¹ dexmedetomidine, respectively.⁸ On the contrary, it was 0.748 ng · ml⁻¹ in the study by Wang *et al.*⁷ after intranasal administration of 1 μg · kg⁻¹ dexmedetomidine. In the current study, the average C_{max} values were 0.499, 0.525, and 0.506 ng · ml⁻¹ for the infant, 1-year-old, and 2-year-old groups, respectively. The simulated intranasal dexmedetomidine C_{max} values of 0.563 ng · ml⁻¹ at 2 μg · kg⁻¹ and 0.260 ng · ml⁻¹ at 1 μg · kg⁻¹ were consistent with those reported by Miller *et al.*⁸ with a similar age group. However, they were lower

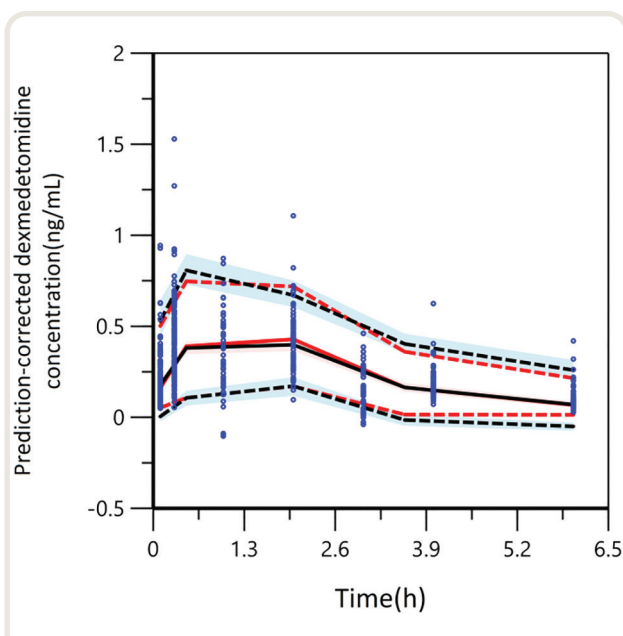


Fig. 2. Prediction-corrected visual predictive check obtained from 1,000 simulations of the database. The *blue circles* represent the prediction corrected plasma concentrations. The *red solid line* in the middle represents the median prediction corrected plasma concentration, and the corresponding *semi-transparent red field* represents a simulation based 95% confidence interval for the median. The 5% and 95% percentiles are presented with the *dashed red lines* in the bottom and upper, and the 95% confidence intervals for the corresponding model predicted percentiles are shown as *semi-transparent blue fields*.

than that in the study by Wang *et al.*⁷ The discrepancy in the results might be attributed to the patients' age range and clinical status as well as the bioavailability of dexmedetomidine by different administration methods.²⁷ Wang *et al.*⁷ recruited older children who underwent different surgeries. In contrast, we enrolled only relatively healthy children with simple vascular malformations in the current study. Dexmedetomidine was administered into the nose by simple drops in the study by Wang *et al.*, whereas an atomization device was used in the study by Miller *et al.* and our study. Although no notable difference was found between administration by an atomizer or by drops in adult volunteers and children,^{4,5} these studies were performed on awake patients in different positions. The bioavailability resulting from different administration methods in anesthetized children would warrant further clarification.

The pharmacokinetic model of intranasal dexmedetomidine was established using an allometric two-compartment disposition model. Clearance changes relatively with weight and organ maturation. Considering the collinearity of weight and age, the use of the allometric scaled model combined with a sigmoidal maturation function facilitated the prediction of mature adult value (70 kg) for comparison across studies. Allometric scaling with an exponent of 0.75

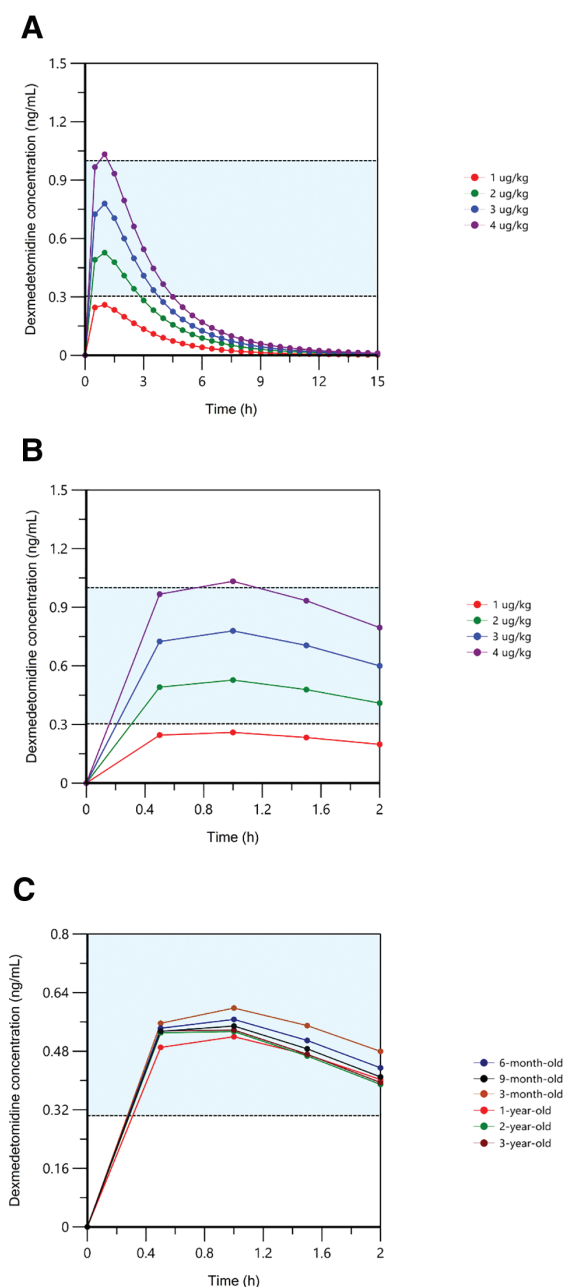


Fig. 3. Simulated pharmacokinetic profiles of the typical pediatric patients under different dosage regimens. The simulated plasma concentration-time curves of 1–4 $\mu\text{g}\cdot\text{kg}^{-1}$ for children (postmenstrual age 101 weeks, weight 10 kg) are shown in *A* (0–15 h) and *B* (0–2 h). The simulated plasma concentration-time curves receiving 2 $\mu\text{g}\cdot\text{kg}^{-1}$ intranasal dexmedetomidine are shown in *C*: (*A*) a 3-month-old child (postmenstrual age 53 weeks, body weight 6.8 kg), (*B*) a 6-month-old child (postmenstrual age 66 weeks, body weight 8.4 kg), (*C*) a 9-month-old child (postmenstrual age 79 weeks, body weight 9.3 kg), (*D*) a 1-y-old child (postmenstrual age 92 weeks, body weight 10.1 kg), (*E*) a 2-y-old child (postmenstrual age 144 weeks, body weight 12.5 kg), (*F*) a 3-y-old child (postmenstrual age 196 weeks, body weight 14.7 kg). The *blue shaded area* represents the target therapeutic window in this study.

AQ23

Table 4. Comparison between Pharmacokinetic Parameters of Intranasal Dexmedetomidine in Children

Pharmacokinetic Parameters	Current Study	Miller <i>et al.</i> ⁸	Wang <i>et al.</i> ⁷
Study population	3–36 mo (n = 137)	6–48 mo (n = 18)	4–10 yr (n = 13)
Systemic clearance (l · h ⁻¹)	9.92	17.88	19.14
Central volume (l)	7.55	3.40	34.2
Intercompartment clearance (l · h ⁻¹)	61.68	41.88	600
Peripheral volume (l)	7.80	16.99	34.9
Absorption rate constant (h ⁻¹)	1.47	0.92	2.27
Lag time (h)	0.021	0.051	—
Bioavailability (%)	—	83.8	—
TM ₅₀ (wk)	46.5	—	—
γ	2.85	—	—

The current study represents children with postmenstrual age 101 weeks and body weight 10 kg; the pharmacokinetic parameters reported by Miller *et al.* represent children with 27-month-old and 12.5 kg.

AQ21

describes drug clearance in children over 2 yr of age, but the allometric exponent then tends to rise with decreasing age.²⁸ Several different methods have been suggested to account for this trend, but they have produced a similar model fit.¹² We found that the scaled allometric model fit our data better than the linear model. Therefore, we chose the sigmoidal maturation function plus allometric scaling as was used in the study by Potts *et al.* so that parameters could easily be compared.²⁹

The bioavailability of intranasal dexmedetomidine by atomizer was 83.8% with a systemic clearance of 62.4 l · h⁻¹ per 70 kg in 6- to 44-month-old children,⁸ whereas the bioavailability was 40.6 to 82% with a systemic clearance of 33.9 to 44 l · h⁻¹ per 70 kg in healthy adults.^{4,30} However, the drug dexmedetomidine in the study by Yoo *et al.*³⁰ was a more concentrated veterinary formulation, and they used nasal spray instead of the conventional atomization or simple drops for drug administration. Therefore, the bioavailability in the study by Yoo *et al.* is not comparable. As age-related dexmedetomidine clearances have been demonstrated by Potts *et al.* using both allometric and linear models,⁹ our apparent clearances estimates were lower than those estimated in older children²⁹ and healthy adults,^{4,30} but similar to those reported in the studies by Miller *et al.* and Wang *et al.*^{7,8} The terminal elimination parameters in our study are also consistent with the studies by Miller *et al.* and Wang *et al.* with a 1.8-h terminal half-life. Ebert *et al.* reported significant changes in cardiac output and heart rate at plasma concentrations of dexmedetomidine that exceeded 1.2 ng · ml⁻¹.³¹ Although body size and age are the two main factors contributing to clearance parameter variability, the hemodynamic effects on clearance under a high dosage of intravenous dexmedetomidine (1 to 6 μg · kg⁻¹) in the study by Potts *et al.*²⁹ are still worthy of attention. In the study by Potts *et al.*, data were pooled from four separate studies, including those involving patients who underwent different types of surgery, which could contribute to the discrepancy.

Compared with empirical sampling, optimal design in conjunction with simulation scenarios has been proven to improve the precision and accuracy of the pharmacokinetic parameters of dexmedetomidine.^{9,32} In this study, we used PopED in R language to determine the optimal design and produce maximal information in pharmacokinetic analysis by providing a strategic sampling schedule with a reduced number of subjects and sampling points in a population of infants and young children. Five blood samples from the three groups were obtained within each optimal sampling window using the D-optimal method. The final pharmacokinetic model provided good accuracy and robustness, with variability ranging from 5 to 21%.

Adult data suggested that dexmedetomidine-mediated sedation and analgesia were dose-dependent.³³ Kim *et al.* found that the effect-site concentration of dexmedetomidine is strongly correlated with the depth of sedation.³⁴ They reported that concentrations of 0.57, 0.89, and 1.19 ng · ml⁻¹ were associated with mild, moderate, and deep levels of sedation, respectively. The target effect-site concentration between 0.2 and 0.4 ng · ml⁻¹ resulted in a significant level of sedation in healthy volunteers.^{35,36} Potts *et al.* reported that children were aroused from dexmedetomidine infusion sedation at a plasma concentration of 0.304 ng · ml⁻¹, and adequate sedation for children in intensive care units was associated with plasma concentrations of 0.4 and 0.8 ng · ml⁻¹ for moderate and deep sedation, respectively.^{9,29} Based on these target concentration values, a dexmedetomidine plasma concentration between 0.3 and 1.0 ng · ml⁻¹ was set as the estimated therapeutic window to produce adequate sedation in our pediatric cohort after general anesthesia.

The simulation results revealed that intranasal administration at 2 μg · kg⁻¹ dexmedetomidine would reach a plasma level of 0.45 ng · ml⁻¹ at 20 min after administration, whereas 3 μg · kg⁻¹ would achieve a plasma level of 0.66 ng · ml⁻¹. Hence, the usual dose of 2 μg · kg⁻¹ or above would be associated with moderate and deep sedation at 20 min after

drug administration. These doses would be adequate for nonpainful procedural sedation that lasts for up to 2 h. The simulated C_{\max} obtained by intranasal dexmedetomidine at 3 to 4 $\mu\text{g} \cdot \text{kg}^{-1}$ (0.780 to 1.03 $\text{ng} \cdot \text{ml}^{-1}$) would be similar to intravenous dexmedetomidine between 1 and 2 $\mu\text{g} \cdot \text{kg}^{-1}$ (0.783 to 1.24 $\text{ng} \cdot \text{ml}^{-1}$).^{8,37} Future pharmacokinetic studies are warranted to validate whether a higher dose of intranasal dexmedetomidine would show dose proportionality, as we have assumed in our simulations. This protocol could be transferred into dose-effect-supportive software and guide individualized treatment in clinical practice.

Nevertheless, this study has several limitations. First, although conventional covariates were evaluated, they did not influence the pharmacokinetic parameters. The probable reason was that we enrolled relatively healthy patients whose baseline laboratory values were almost normal. Given that dexmedetomidine is metabolized primarily by *UGTs* (*UGT1A4* and *UGT2B10*) and *CYPs* (*CYP2A6*), information on its pharmacogenetics was not available in this study. Second, despite having used an optimized method for sampling design, the current data did not produce stable K_a and lag time estimates. Third, as intravenous dexmedetomidine administration was not included in this study, the bioavailability of intranasally administered dexmedetomidine was not estimated. Last, the simulations in our study were based on the assumption that the PK profile was linear concerning the dose. However, the absorption of intranasal dexmedetomidine in children is related to the nasal mucosal surface area and anatomy. These factors might be associated with lower bioavailability and behave differently at high dosages, and point to a need for further intranasal dose-ranging studies.

Conclusions

Using an optimal sampling schedule in conjunction with allometrically scaled and maturation models, pharmacokinetic parameters of intranasal dexmedetomidine for children aged 3 months to 3 yr were comprehensively evaluated. Model simulations indicated that intranasal administration at 2 $\mu\text{g} \cdot \text{kg}^{-1}$ dexmedetomidine would be associated with mild to moderate sedation within 20 min, and C_{\max} would be achieved at 61 min. This dose would be feasible for nonpainful procedural sedation that lasts for up to 2 h. An increase in dosage might increase maximum concentrations and prolong the duration of sedation. Model simulations with different dosages should be applied to predict individualized dosing regimens and help to reduce the potential adverse effects associated with overdose.

Acknowledgments

The authors gratefully acknowledge the assistance of Ao Zheng, Department of Anesthesiology, Guangzhou Women and Children's Medical Center, Guangzhou, China, for his assistance as a research coordinator in this study. The authors

also gratefully acknowledge the assistance of Yao Liu, Si Y. Wang, and Fu L. Jiang, Institute of Clinical Pharmacology, School of Pharmaceutical Sciences, Sun Yat-Sen University, Guangzhou, China, for plasma concentration determination and data analysis of the study.

Research Support

This work was supported by the National Natural Science Foundation of China (China; grant No. 81901385), National Key Research and Development Program of China during the 13th 5-yr plan (China; grant No. 2018ZX09734-003), and Guangzhou Women and Children's Medical Center/Guangzhou Institute of Pediatrics (China; grant No. Pre-PI-2019-011).

Competing Interests

The authors declare no competing interests.

Reproducible Science

Full protocol available at: sxjess@126.com. Raw data available at: sxjess@126.com

Correspondence

Address correspondence to Dr. Song: Department of Anesthesiology, Guangzhou Women and Children's Medical Center and Guangzhou Medical University, Guangzhou, Guangdong, China. sxjess@126.com. ANESTHESIOLOGY's articles are made freely accessible to all readers on www.anesthesiology.org, for personal use only, 6 months from the cover date of the issue.

References

1. Poonai N, Spohn J, Vandermeer B, Ali S, Bhatt M, Hendriks S, Trottier ED, Sabhaney V, Shah A, Joubert G, Hartling L: Intranasal dexmedetomidine for procedural distress in children: A systematic review. *Pediatrics* 2020; 145:e20191623
2. Yuen VM, Hui TW, Irwin MG, Yao TJ, Wong GL, Yuen MK: Optimal timing for the administration of intranasal dexmedetomidine for premedication in children. *Anaesthesia* 2010; 65:922-9
3. Yuen VM, Irwin MG, Hui TW, Yuen MK, Lee LH: A double-blind, crossover assessment of the sedative and analgesic effects of intranasal dexmedetomidine. *Anesth Analg* 2007; 105:374-80
4. Li A, Yuen VM, Goulay-Dufay S, Sheng Y, Standing JF, Kwok PCL, Leung MKM, Leung AS, Wong ICK, Irwin MG: Pharmacokinetic and pharmacodynamic study of intranasal and intravenous dexmedetomidine. *Br J Anaesth* 2018; 120:960-8
5. Li BL, Zhang N, Huang JX, Qiu QQ, Tian H, Ni J, Song XR, Yuen VM, Irwin MG: A comparison of intranasal

- dexmedetomidine for sedation in children administered either by atomiser or by drops. *Anaesthesia* 2016; 71:522–8
6. Yuen VM, Hui TW, Irwin MG, Yao TJ, Chan L, Wong GL, Shahnaz Hasan M, Shariffuddin II: A randomised comparison of two intranasal dexmedetomidine doses for premedication in children. *Anaesthesia* 2012; 67:1210–6
 7. Wang CY, Ihmsen H, Hu ZY, Chen J, Ye XF, Chen F, Lu Y, Schüttler J, Lian QQ, Liu HC: Pharmacokinetics of intranasally administered dexmedetomidine in Chinese children. *Front Pharmacol* 2019; 10:756
 8. Miller JW, Balyan R, Dong M, Mahmoud M, Lam JE, Pratap JN, Paquin JR, Li BL, Spaeth JP, Vinks A, Loepke AW: Does intranasal dexmedetomidine provide adequate plasma concentrations for sedation in children: A pharmacokinetic study. *Br J Anaesth* 2018; 120:1056–65
 9. Potts AL, Warman GR, Anderson BJ: Dexmedetomidine disposition in children: A population analysis. *Paediatr Anaesth* 2008; 18:722–30
 10. Yuen VM, Li BL, Cheuk DK, Leung MKM, Hui TWC, Wong IC, Lam WW, Choi SW, Irwin MG: A randomised controlled trial of oral chloral hydrate vs. intranasal dexmedetomidine before computerised tomography in children. *Anaesthesia* 2017; 72:1191–5
 11. Ni J, Wei J, Yao Y, Jiang X, Luo L, Luo D: Effect of dexmedetomidine on preventing postoperative agitation in children: a meta-analysis. *PLoS One* 2015; 10:e0128450
 12. Germovsek E, Barker CI, Sharland M, Standing JF: Scaling clearance in paediatric pharmacokinetics: All models are wrong, which are useful? *Br J Clin Pharmacol* 2017; 83:777–90
 13. Schwartz GJ, Work DF: Measurement and estimation of GFR in children and adolescents. *Clin J Am Soc Nephrol* 2009; 4:1832–43
 14. Guan Y, Li B, Wei W, Wang S, Yuen VM, Liu Y, Ao Z, Zhou S, Tian H, Huang M, Song X, Zhong G: Quantitative ultra-high-performance liquid chromatography-tandem mass spectrometry for determination of dexmedetomidine in pediatric plasma samples: Correlation with genetic polymorphisms. *Biomed Chromatogr* 2019; 33:e4683
 15. *Bioanalytical Method Validation Guidance for Industry*: Edited by US Department of Health and Human Services FaDA, Center for Drug Evaluation and Research (CDER) and Center for Veterinary Medicine (CVM), 2018
 16. Bergstrand M, Karlsson MO: Handling data below the limit of quantification in mixed effect models. *AAPS J* 2009; 11:371–80
 17. Ahn JE, Karlsson MO, Dunne A, Ludden TM: Likelihood based approaches to handling data below the quantification limit using NONMEM VI. *J Pharmacokinetic Pharmacodyn* 2008; 35:401–21
 18. Anderson BJ, Holford NH: Mechanism-based concepts of size and maturity in pharmacokinetics. *Annu Rev Pharmacol Toxicol* 2008; 48:303–32
 19. Bonate PL: The effect of collinearity on parameter estimates in nonlinear mixed effect models. *Pharm Res* 1999; 16:709–17
 20. Leeder JS, Meibohm B: Challenges and opportunities for increasing the knowledge base related to drug biotransformation and pharmacokinetics during growth and development. *Drug Metab Dispos* 2016; 44:916–23
 21. Karlsson MO, Savic RM: Diagnosing model diagnostics. *Clin Pharmacol Ther* 2007; 82:17–20
 22. van Hoorn CE, Flint RB, Skowno J, Davies P, Engelhardt T, Lalwani K, Olutoye O, Ista E, de Graaff JC: Off-label use of dexmedetomidine in paediatric anaesthesiology: An international survey of 791 (paediatric) anaesthesiologists. *Eur J Clin Pharmacol* 2021; 77:625–35
 23. Li BL, Ni J, Huang JX, Zhang N, Song XR, Yuen VM: Intranasal dexmedetomidine for sedation in children undergoing transthoracic echocardiography study—A prospective observational study. *Paediatr Anaesth* 2015; 25:891–6
 24. Tug A, Hanci A, Turk HS, Aybey F, Isil CT, Sayin P, Oba S: Comparison of two different intranasal doses of dexmedetomidine in children for magnetic resonance imaging sedation. *Paediatr Drugs* 2015; 17:479–85
 25. Li H, Ji CY, Zong XN, Zhang YQ: [Height and weight standardized growth charts for Chinese children and adolescents aged 0 to 18 years]. *Zhonghua Er Ke Za Zhi* 2009; 47:487–92
 26. Palaparthi R, Rehman MI, von Richter O, Yin D: Population pharmacokinetics of PF-06438179/GP1111 (an infliximab biosimilar) and reference infliximab in patients with moderately to severely active rheumatoid arthritis. *Expert Opin Biol Ther* 2019; 19:1065–74
 27. Holliday SF, Kane-Gill SL, Empey PE, Buckley MS, Smithburger PL: Interpatient variability in dexmedetomidine response: A survey of the literature. *ScientificWorldJournal* 2014; 2014:805013
 28. Calvier EA, Krekels EH, Väitalo PA, Rostami-Hodjegan A, Tibboel D, Danhof M, Knibbe CA: Allometric scaling of clearance in paediatric patients: When does the magic of 0.75 fade? *Clin Pharmacokinetic* 2017; 56:273–85
 29. Potts AL, Anderson BJ, Warman GR, Lerman J, Diaz SM, Vilo S: Dexmedetomidine pharmacokinetics in pediatric intensive care—A pooled analysis. *Paediatr Anaesth* 2009; 19:1119–29
 30. Yoo H, Iirola T, Vilo S, Manner T, Aantaa R, Lahtinen M, Scheinin M, Olkkola KT, Jusko WJ: Mechanism-based

- population pharmacokinetic and pharmacodynamic modeling of intravenous and intranasal dexmedetomidine in healthy subjects. *Eur J Clin Pharmacol* 2015; 71:1197–207
31. Ebert TJ, Hall JE, Barney JA, Uhrich TD, Colino MD: The effects of increasing plasma concentrations of dexmedetomidine in humans. *ANESTHESIOLOGY* 2000; 93:382–94
 32. van Dijkman SC, De Cock PAJG, Smets K, Decaluwe W, Smits A, Allegaert K, Vande Walle J, De Paepe P, Della Pasqua O: Dose rationale and pharmacokinetics of dexmedetomidine in mechanically ventilated new-borns: Impact of design optimisation. *Eur J Clin Pharmacol* 2019; 75:1393–404
 33. Mohamed SA, Abdel-Ghaffar HS, Hassan NA, El Sherif FA, Shouman SA, Omran MM, Hassan SB, Allam AAAE, Sayed DG: Pharmacokinetics and pharmacodynamics of 3 doses of oral-mucosal dexmedetomidine gel for sedative premedication in women undergoing modified radical mastectomy for breast cancer. *Anesth Analg* 2021; 132:456–64
 34. Kim KM, Seo KH, Lee JM, Park EY, Park J: Target-controlled infusion of dexmedetomidine effect-site concentration for sedation in patients undergoing spinal anaesthesia. *J Clin Pharm Ther* 2020; 45:347–53
 35. Colin PJ, Hannivoort LN, Eleveld DJ, Reyntjens KMEM, Absalom AR, Vereecke HEM, Struys MMRF: Dexmedetomidine pharmacokinetic-pharmacodynamic modelling in healthy volunteers: 1. Influence of arousal on Bispectral Index and sedation. *Br J Anaesth* 2017; 119:200–10
 36. Bloor BC, Ward DS, Belleville JP, Maze M: Effects of intravenous dexmedetomidine in humans. II. Hemodynamic changes. *ANESTHESIOLOGY* 1992; 77:1134–42
 37. Anttila M, Penttilä J, Helminen A, Vuorilehto L, Scheinin H: Bioavailability of dexmedetomidine after extravascular doses in healthy subjects. *Br J Clin Pharmacol* 2003; 56:691–3